

Ultra-rapid microwave synthesis of triplite  $\text{LiFeSO}_4\text{F}$ Cite this: *J. Mater. Chem. A*, 2013, **1**, 2990Rajesh Tripathi,<sup>a</sup> Guerman Popov,<sup>a</sup> Xiaoqi Sun,<sup>a</sup> Dominic H. Ryan<sup>b</sup> and Linda F. Nazar<sup>\*a</sup>Received 8th November 2012  
Accepted 7th December 2012

DOI: 10.1039/c2ta01022d

www.rsc.org/MaterialsA

Quick, effective synthesis of the 4 V Li-ion battery cathode material, triplite  $\text{LiFeSO}_4\text{F}$ , takes place *via* facile conversion of the defect-peppered nanocrystalline tavorite precursor that forms on ultra-rapid microwave heating (10 min) of  $\text{FeSO}_4 \cdot \text{H}_2\text{O}/\text{LiF}$ . We propose a mechanism for its unique phase transformation to the triplite that occurs as a consequence of the disorder and hydroxyl defects induced by the fast nucleation. The electrochemical properties of the resultant triplite exhibits a doubling of its practical gravimetric capacity compared to the material prepared by conventional methods.

High (~4 V) voltage positive electrode materials are key for success of Li-ion batteries to increase the available energy density storage. Due to their high practical and academic significance they remain a highly investigated material group.<sup>1,2</sup> It is also important that materials are inexpensive and environmentally friendly, and Fe-based materials such as olivine phosphates that have been recently commercialized are attractive in this respect. Although their energy density suffers from an intermediate-energy redox couple voltage (3.4 V), this can be significantly improved with Mn substitution, albeit with some loss in rate capability.<sup>3,4</sup>

Another highly viable substitution target is the anion. Both hydroxysulphates<sup>5</sup> and fluorosulphates have been examined, where the latter offer an increase in voltage *vis a vis* phosphates<sup>6,7</sup> owing to the polarizing effect of the  $\text{F}^-$  ion (which can raise the potential compared to  $\text{O}^{2-}$ ), and to the greater electron withdrawing nature of the sulfate group based on the well known “inductive” covalent bonding effect proposed by Goodenough well over a decade ago. Substitution of sulfate ( $\text{SO}_4$ )<sup>2-</sup> moieties in place of phosphate ( $\text{PO}_4$ )<sup>3-</sup> moieties in isostructural NASICON frameworks, for example, can increase the open circuit voltage by 0.8 V, thus increasing the overall energy density.<sup>8</sup> The change in anion also

results in a very significant change in structure. The synthesis of the favorite polymorph of  $\text{LiFeSO}_4\text{F}$  was first accomplished in 2010 using either low temperature ionothermal<sup>6</sup> or solvothermal chemistry.<sup>9</sup> It exhibits a triclinic structure that remains very similar on Li extraction despite a small change in symmetry. In contrast,  $\text{LiMnSO}_4\text{F}$  adopts a triplite framework that is completely redox inactive, which is related to tavorite except the Li and Mn are completely disordered over two sites;<sup>10</sup> this structure is maintained on Fe substitution up to 80–90% but the material exhibits excellent redox activity.<sup>11,13</sup> Recently, it has been shown that the pure iron triplite phase  $\text{LiFeSO}_4\text{F}$  is also accessible *via* solid state reactions.<sup>12</sup> It is, furthermore, the more thermodynamically stable phase: it can be accessed *via* conversion through the tavorite intermediate, typically by extended reaction at intermediate temperatures.<sup>13</sup> The Fe triplite (de)intercalates Li at 3.9 V, which is 0.3 V higher than its ordered tavorite analogue, attributable to its longer average Fe–O bond length. However, the mobility of Li ions in triplite is lower owing to the Fe/Li disorder in the lattice, and reversible capacities of only up to 0.45 Li/Fe have been reported for conventionally prepared materials.<sup>12</sup>

Development of new synthetic methods in this class of materials that can access improved materials is thus paramount for better electrochemical behavior. However, the metastability and moisture sensitivity of  $\text{LiFeSO}_4\text{F}$  pose challenges. Herein we address these by using a gentle microwave solvothermal technique which generates the precursor tavorite phase from the reaction of  $\text{FeSO}_4 \cdot \text{H}_2\text{O}$  and LiF in 10 minutes. The ultra-rapid process results in homogeneously sized nanocrystallites with considerable lattice microstrain. They are readily converted to  $\text{LiFeSO}_4\text{F}$  triplite on heating, by means of an unusual phase transformation mechanism that relies on defects within the lattice to facilitate the conversion. Lattice defects such as spinel  $\text{LiMn}_2\text{O}_4$  nanodomains in rock salt  $\text{Li}_2\text{MnO}_3$  (ref. 14) have been shown to accelerate phase transformations in oxide materials, but this has not yet been demonstrated in the polyanion family of materials to our knowledge. The resultant triplite displays significantly improved electrochemical behavior.

Microwave solvothermal reactions<sup>15</sup> developed over the last two decades have been used to prepare cathode materials that include

<sup>a</sup>Department of Chemistry, University of Waterloo, 200 University Avenue West, Waterloo, ON, N2L 3G1, Canada. E-mail: lfnazar@uwaterloo.ca

<sup>b</sup>Physics Department, McGill University, Montreal, QC, H3A 2T8, Canada

† Electronic supplementary information (ESI) available. See DOI: 10.1039/c2ta01022d

olivine phosphates, oxides and silicates.<sup>16–19</sup> We chose tetraethylene glycol (TEG) as a reaction medium because polyols are heated by microwaves very quickly due to their high loss tangent,<sup>20</sup> and an Anton Paar Synthos 3000 system to allow for software control and continuous monitoring of the desired microwave exposure time and temperature. Fig. 1a shows a selected region of the XRD pattern of the initial  $\text{LiFeSO}_4\text{F}$  prepared by this method. The characteristic reflections identify it as phase-pure tavorite, and clearly differentiate it from the starting material,  $\text{FeSO}_4 \cdot \text{H}_2\text{O}$ . The SEM image (see ESI, Fig. S1a†) shows particles with sizes ranging from 100 to 200 nm. The Mössbauer spectrum (see ESI, Fig. S2†) was fit with two  $\text{Fe}^{2+}$  doublets of equal contribution in accord with the known crystal structure,<sup>6</sup> with no trace of  $\text{Fe}^{3+}$ . Significant broadening of the outer doublet peaks is indicative of local disorder. The XRD pattern also exhibits noticeably broader peaks compared to those of the conventional solvothermal tavorite (“ST tavorite”, Fig. 1b). X-ray diffraction data analysis was carried out using Bruker TOPAS 4.2 software using the fundamental parameters approach. The refined parameters CS\_L (crystallite size) and Strain\_L (microstrain) corresponding to a Lorentzian convolution were 53(4) and 0.44(4) respectively for the microwave tavorite (“MW tavorite”), whereas the same parameters for the ST tavorite were 87(7) and 0.21(2) (see ESI, Fig. S3†). While the crystallite size parameter (*i.e.*, coherent scattering domain size) is 1.5 times lower for the MW tavorite, its microstrain parameter is twofold higher, indicating that microstrain is the major contributor to peak broadening due to defects within the lattice.

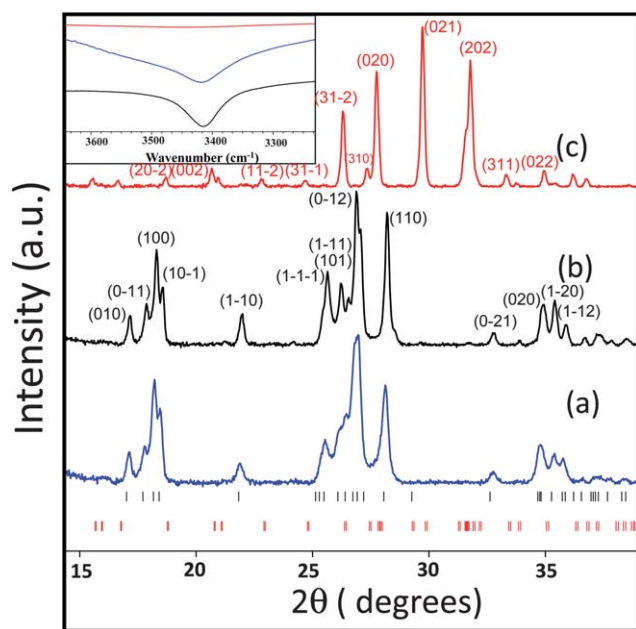


**Fig. 1** X-ray diffraction pattern ( $\text{Cu-K}\alpha$  radiation,  $\lambda = 1.5406 \text{ \AA}$ ) of: (a) MW tavorite  $\text{LiFeSO}_4\text{F}$  prepared by the microwave solvothermal method; (b) ST tavorite  $\text{LiFeSO}_4\text{F}$  prepared by a conventional solvothermal method; (c) triplite  $\text{LiFeSO}_4\text{F}$  prepared by heat treatment of the MW-tavorite. The lower black markers represent the phase markers for tavorite  $\text{LiFeSO}_4\text{F}$  and the red markers represent the phase markers for triplite  $\text{LiFeSO}_4\text{F}$ . Miller indices for (a) are the same as for (b). FTIR spectra are shown in the inset. The same color code is used for the FTIR and XRD data.

The high amount of microstrain we observe in the precursor tavorite is attributed to its rapid synthesis that leads to disorder. Glycol media are known to strongly interact with microwave radiation *via* a dipolar–microwave interaction mechanism which leads to rapidly superheated local regions in the reaction medium.<sup>21</sup> This will increase the exchange rate of the H–OH molecules with Li–F in  $\text{FeSO}_4 \cdot \text{H}_2\text{O}$  (*i.e.*,  $\text{HFeSO}_4\text{OH}$ ) that defines the topotactic reaction that forms tavorite  $\text{LiFeSO}_4\text{F}$ .<sup>6</sup> This reaction clearly must start at the crystallite surface that is in contact with LiF in solution, followed by migration of the phase front deeper into the precursor particle as the reaction progresses. The tavorite crystallites break off from the parent particle when the stress associated with the volume difference of the two phases at the boundary exceeds a given limit. In contrast to conventional solvothermal methods where slow heating mainly occurs *via* thermal conduction mechanisms, heating of the entire reaction zone by penetration of the microwaves<sup>21</sup> can simultaneously trigger the topotactic reaction at many points on the precursor crystallite surface, causing rapid, multiple fragmentation. The result we observe is both small tavorite nanocrystallites ( $\sim 150$  to  $200 \text{ nm}$ ) and inhomogeneous reactivity that leads to a minor fraction of crystallite defects in the form of hydroxyl groups (and possibly other) as discussed below.

Although continued microwave heating of the tavorite in glycol media up to  $300 \text{ }^\circ\text{C}$  for 3 hours did not result in conversion to triplite, the phase transformation was effected by a very short solid-state heat treatment ( $<60 \text{ min}$ ) of the MW tavorite  $\text{LiFeSO}_4\text{F}$  at  $350 \text{ }^\circ\text{C}$  as indicated by the XRD pattern shown in Fig. 1c. Tavorite  $\text{LiFeSO}_4\text{F}$  samples prepared by other methods do not undergo such rapid conversion. Furthermore, coating the MW tavorite with a carbonaceous coating – by mixing it with sucrose (2 : 1 wt ratio) and heating for  $350 \text{ }^\circ\text{C}$  for 1 h – retards the loss of the hydroxyl groups (see below), and delays the phase transformation. Namely, the XRD pattern of the coated/heated material initially only showed reflections of tavorite, although gradual conversion to the triplite polymorph did occur after 8 hours. Triplite can also be obtained by slow reaction in glycol at  $250 \text{ }^\circ\text{C}$  that converts tavorite  $\text{LiFeSO}_4\text{F}$  to the triplite polymorph over a period of two weeks.<sup>13</sup> The tavorite prepared by conventional solvothermal methods does not show any phase transformation after heat treatment ( $350 \text{ }^\circ\text{C}$ ) until 12 h, after which the phase transformation is accompanied by a significant formation of extraneous iron oxides (see ESI, Fig. S4†). These impurities have also been reported to form during direct solid state synthesis of the triplite  $\text{LiFeSO}_4\text{F}$  using an intimately mixed stoichiometric ratio of LiF and  $\text{FeSO}_4 \cdot \text{H}_2\text{O}$ .<sup>22</sup> No impurities are visible in the XRD pattern of the triplite sample obtained by the microwave route (Fig. 1c). This suggests that the pathway governing the conversion of tavorite to triplite is greatly facilitated, providing an easy scalable route for the synthesis of phase-pure material.

Fig. 1 (inset) shows FTIR spectra collected for both tavorite and triplite  $\text{LiFeSO}_4\text{F}$  synthesized using either microwave or conventional solvothermal methods, in the frequency range between  $3200$  and  $3600 \text{ cm}^{-1}$  that corresponds to the vibration modes of  $\text{OH}^-$  species (see ESI, Fig. S5† for the full-range spectra). Hydroxyl bands are present in both of the tavorite samples. In the microwave prepared sample, however, the broad peaks around  $3400 \text{ cm}^{-1}$  are ascribed to residual solvent TEG,<sup>23</sup> whereas the shoulder at  $\sim 3600 \text{ cm}^{-1}$  indicates the presence of framework  $\text{OH}^-$  groups that

typically lie between 3700 and 3500  $\text{cm}^{-1}$  in hydroxysulphates.<sup>24</sup> The presence of hydroxyl groups is supported by elastic recoil detection (ERD) analysis of a pressed pellet of MW tavorite that provided a hydrogen content of between 2.5–3.5 atomic%, based on a fit of the ERD data to a model comprising a hydrogen gradient that is slightly higher on the pellet surface (see ESI, Fig. S6†). On conversion to triplite, the framework  $\text{OH}^-$  disappear. In contrast, hydroxyl groups are not visible in conventional solvothermal tavorite which shows only a typical surface glycol peak<sup>23</sup> contribution at  $\sim 3400 \text{ cm}^{-1}$ . Thus, the microwave tavorite is characterized by a hydroxyl contribution that disappears upon conversion to triplite, whereas this feature is absent for the conventional solvothermal tavorite. The highly kinetically favored phase transition of the tavorite  $\text{LiFeSO}_4\text{F}$  samples synthesized by the microwave solvothermal route can be explained by the introduction of significant defects this induces.

The target end product – MW  $\text{LiFeSO}_4\text{F}$  triplite – was examined by both Mössbauer spectroscopy and powder neutron and X-ray diffraction, which demonstrated that a very well crystallized material was formed. We fit the Mössbauer spectra using two high spin  $\text{Fe}^{2+}$  doublets of exactly equal areas in accord with the two iron sites in the structure (see ESI, Fig. S2†), unlike previous reports where a three-site parameter fit was employed suggestive of additional lattice contributions.<sup>11</sup> The combined neutron and X-ray Rietveld refinement also converged with excellent “goodness of fit” parameters ( $R_{\text{wp}} = 1.95\%$ ,  $\chi^2 = 1.94$ , see ESI, Table S1†). The fit results do not show any anomalies (Fig. 2) and the obtained structural and thermal parameters are reasonable and in full accord with those

reported elsewhere for the iron triplite.<sup>13</sup> Neutron diffraction shows that there is no significant ordering of Li and Fe on the two sites as expected, although Li has a slight preference towards site 2 [specifically, 0.426(2) Li (site 1)/0.574(2) Li (site 2)]. The higher entropy associated with the disordered nature of the Li and Fe sites results in triplite being the thermodynamically preferred polymorph of  $\text{LiFeSO}_4\text{F}$ , as we discussed previously.<sup>13</sup> This has been recently confirmed by detailed calorimetric studies.<sup>25</sup>

The inherent microstrain and defect-induced disorder in the precursor MW tavorite provide several factors that can lower the activation energy for its conversion to the triplite phase. Although the MW tavorite exhibits a relatively small crystallite size ( $\sim 200 \text{ nm}$ ), this is unlikely to be an influence on the kinetics of transformation, since ionothermally synthesised tavorite of similar or smaller dimensions does not undergo ready conversion to triplite.<sup>11</sup> However, disorder in the precursor will certainly favour the product triplite, which possesses intrinsic disorder. The disorder in the tavorite precursor can take the form of structural defects, and/or the hydroxyl groups whose loss upon solid state conversion to triplite is indeed a factor. The latter is suggested by the fact that the transformation occurs very slowly at 250–300 °C in glycol (as opposed to an argon flow): namely over the period of weeks, not minutes. Deliberate blocking of the surface also slows down the phase transformation (*vide supra*). We note that release of the hydroxyl groups on heating may proceed *via* a complex pathway. We base this on thorough studies of the dehydration of isostructural  $\text{FePO}_4 \cdot \text{H}_2\text{O}$  (*i.e.*,  $\text{HFePO}_4\text{OH}$ ) to  $\text{FePO}_4$ , where the formation of new intermediate ordered phases with iron vacancies and contracted cell volumes has been demonstrated.<sup>26</sup> Although the fraction of such phases would be far too low in our case to be detected (owing to the  $\sim 3\%$  hydroxyl content), their formation as a low concentration of nanodomains could provide empty iron sites that would enhance  $\text{Li}^+$  migration and  $\text{Li}^+/\text{Fe}^{2+}$  site exchange that favour triplite phase formation. A further reduction in unit cell volume would result because triplite exhibits a 2.4% lower unit cell volume per formula unit ( $\Delta V/Z$ ) (see ESI† for unit cell parameters). Thus, on the surface where dehydration starts, a radial compressive stress for a spherical particle would be generated that would increase as the reaction

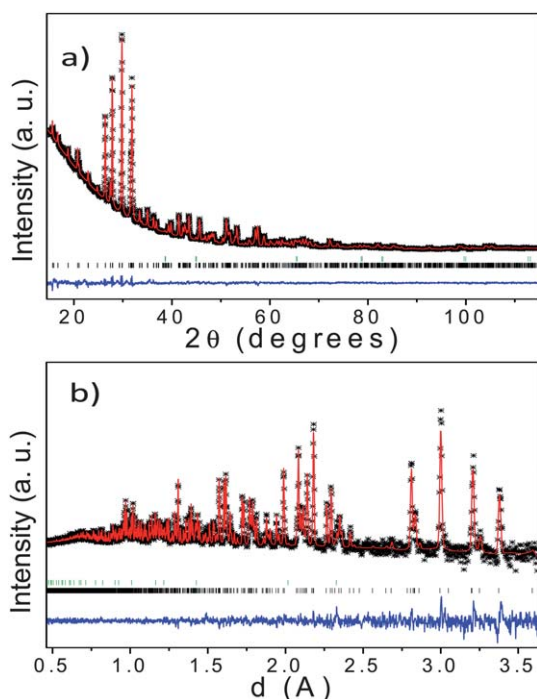


**Fig. 2** Structural refinement of triplite  $\text{LiFeSO}_4\text{F}$ : (a) X-ray diffraction (Cu-K $\alpha$ ); (b) time-of-flight neutron diffraction refinement results. Black points represent experimental data, red solid lines show fitted data, and blue lines show the difference map between the observed and calculated data. Lower black phase markers represent  $\text{LiFeSO}_4\text{F}$ , upper green phase markers correspond to  $\text{LiF}$  (<1 wt % by Rietveld analysis).

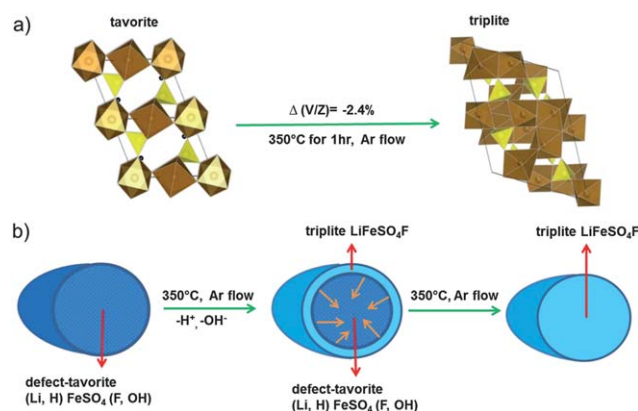


**Fig. 3** (a) A schematic showing the structural transformation of  $\text{LiFeSO}_4\text{F}$  from the tavorite to the triplite phase that is accompanied by a volume contraction; (b) proposed mechanism of the phase transformation of microwave prepared tavorite to triplite.

progresses and provide a trigger for the phase transformation. This stress can be released by transforming the underlying tavorite to the denser atomic packing provided by triplite. Fig. 3 shows a scheme that summarizes this mechanism.

The phase-pure MW triplite that is formed by rapid transformation exhibits superior electrochemical performance to that prepared by other methods, which is not the case for tavorite. For the tavorite shown in Fig. 4a which is the precursor phase to triplite, lithium is reversibly de-/intercalated at 0.1C (0.85 Li) at a characteristic voltage plateau of 3.6 V vs. Li/Li<sup>+</sup>. This performance is quite similar to this material prepared by solvothermal or ionothermal methods.<sup>6,9</sup> In contrast, the electrochemical performance of MW triplite LiFeSO<sub>4</sub>F (Fig. 4b) is greatly improved *vis a vis* other synthetic routes. Nearly 90% of the Li could be extracted on the first cycle (corresponding to a gravimetric capacity of 130 mA h g<sup>-1</sup>), and 80% reversibly intercalated at a C/20 rate, which far exceeds that previously reported for triplite LiFeSO<sub>4</sub>F (~45% Li).<sup>12</sup> This is in part the result of the much smaller crystallite dimensions of about 300–500 nm afforded by the microwave process (see ESI, Fig. S1b and c<sup>†</sup>), which provide shorter pathways for Li-ion transport.<sup>27</sup> In triplite, this is vital because the disorder on the Li/Fe sites increases the activation energy for the Li-ion migration pathways and renders a fraction of Li ions in the core of the material inaccessible at intermediate rates in micron-sized particles.<sup>7</sup> The origin of the initial

sloping profile in triplite evident in Fig. 4b, suggestive of a solid solution regime between 0.8 < x < 1, is currently under detailed investigation.

In conclusion, we have achieved a more complete understanding of the phase transformation of tavorite to the higher energy density triplite phase. Local rapid heating induced by microwave-heating rapidly generates nanocrystalline LiFeSO<sub>4</sub>F tavorite with defects that induce significant microstrain. To date, this is unique to the microwave synthesis method. Phase transformation to the more stable triplite framework, facilitated by the lattice defects which include hydroxyl groups, is therefore easily triggered. The formation of nanocrystalline tavorite leads to nanocrystalline triplite, which greatly favors its electrochemical performance because of the inherently disordered nature of the triplite structure. The ability of ultra-rapid microwave heating to create metastable disordered crystalline materials is an important factor to consider when employing this approach to create new materials. When highly ordered materials are ultimately desired this may initially seem to be a liability. However, it can also provide a unique route to lower the activation energy of phase transformations to open up a wide range of unique synthetic pathways. It offers a tunable, flexible approach to preassemble materials with thorough “mixing” at the nanoscale that are ideally poised for subsequent reaction. This can allow the access of more stable materials of importance to energy storage without the necessity for high temperature reaction.

## Acknowledgements

LFN gratefully acknowledges NSERC through its Discovery and Strategic funding programs, and the generous support of GM Canada through the NSERC Collaborative Research and Development program. We thank Dr Ashfia Huq for the neutron diffraction data that were collected at the Oak Ridge National Laboratory's Spallation Neutron Source; research sponsored by the Scientific User Facilities Division, Office of Basic Energy Sciences, U.S. Department of Energy. We thank Professor Lyudmila Goncharova of Department of Physics and Astronomy, Western University, London, Ontario, Canada for the ERD analysis.

## References

- 1 B. L. Ellis, K. T. Lee and L. F. Nazar, *Chem. Mater.*, 2010, **22**, 691–714.
- 2 M. Armand and J.-M. Tarascon, *Nature*, 2008, **451**, 652–657.
- 3 S.-M. Oh, S.-T. Myung, J. B. Park, B. Scrosati, K. Amine and Y.-K. Sun, *Angew. Chem., Int. Ed.*, 2012, **51**, 1853–1856.
- 4 G. R. Gardiner and M. S. Islam, *Chem. Mater.*, 2010, **22**, 1242–1248.
- 5 M. A. Reddy, V. Pralong, V. Caignaert and B. Raveau, *Electrochem. Commun.*, 2009, **11**, 1807–1810.
- 6 N. Recham, J. N. Chotard, L. Dupont, C. Delacourt, W. Walker, M. Armand and J.-M. Tarascon, *Nat. Mater.*, 2010, **9**, 68–74.
- 7 R. Tripathi, G. R. Gardiner, M. S. Islam and L. F. Nazar, *Chem. Mater.*, 2011, **23**, 2278–2284.
- 8 A. K. Padhi, M. Manivannan and J. B. Goodenough, *J. Electrochem. Soc.*, 1998, **145**, 1518–1523.

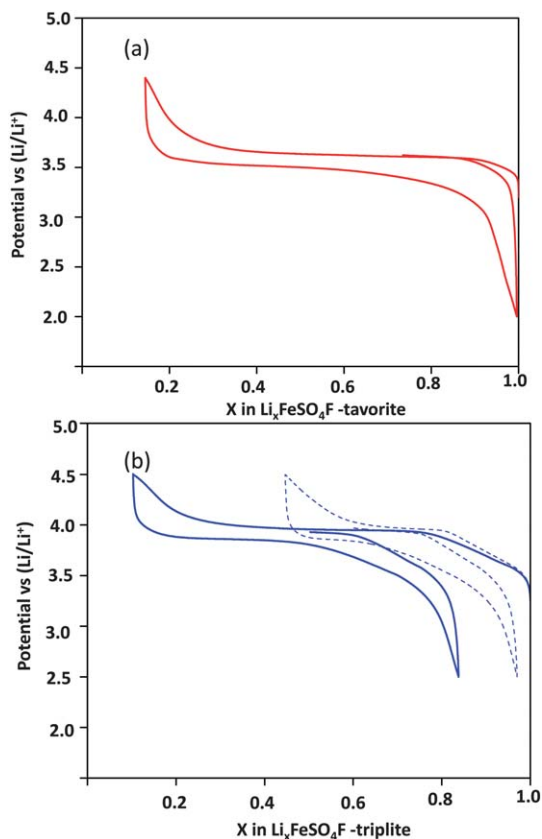


**Fig. 4** Charge–discharge voltage profiles (first and second cycles) of (a) microwave prepared tavorite LiFeSO<sub>4</sub>F at a C/10 rate in the voltage window from 2.0–4.5 V; (b) triplite LiFeSO<sub>4</sub>F prepared by heating microwave tavorite (solid line) and triplite prepared by extended conventional solvothermal method (dotted curve) in the voltage window from 2.5–4.5 V at a C/20 rate.

- 9 R. Tripathi, T. N. Ramesh, B. L. Ellis and L. F. Nazar, *Angew. Chem., Int. Ed.*, 2010, **49**, 8738–8742.
- 10 L. Waldrop, *Naturwissenschaften*, 1968, **118**, 178–179.
- 11 P. Barpanda, M. Ati, B. C. Melot, G. Rousse, J.-N. Chotard, M.-L. Doublet, M.-T. Sougrati, S.-A. Corr, J.-C. Jumas and J.-M. Tarascon, *Nat. Mater.*, 2011, **10**, 772–779.
- 12 M. Ati, B. C. Melot, J. N. Chotard, G. Rousse, M. Reynaud and J. M. Tarascon, *Electrochem. Commun.*, 2011, **13**, 1280–1283.
- 13 R. Tripathi, G. Popov, B. L. Ellis, A. Huq and L. F. Nazar, *Energy Environ. Sci.*, 2012, **5**, 6238–6246.
- 14 A. Boulineau, L. Croguennec, C. Delmas and F. Weill, *Dalton Trans.*, 2012, **41**, 1574–1581.
- 15 M. Baghbanzadeh, L. Carbone, P. D. Cozzoli and C. O. Kappe, *Angew. Chem. Int. Ed.*, 2011, **50**, 2–50.
- 16 A. V. Murugan, T. Muraliganth and A. Manthiram, *Electrochem. Commun.*, 2008, **10**, 903–906.
- 17 T. Muraliganth, K. R. Stroukoff and A. Manthiram, *Chem. Mater.*, 2010, **22**, 5754–5761.
- 18 Y. Sukeun, L. Eun-Sung and A. Manthiram, *Inorg. Chem.*, 2012, **51**, 3505–3512.
- 19 D. Carriazo, M. D. Rossell, G. B. Zeng, I. Bilecka, R. Erni and M. Niederberger, *Small*, 2012, **8**, 2231–2238.
- 20 C. Gabriel, M. Gabriel, H. E. Grant, B. S. J. Halstead and D. M. P. Mingos, *Chem. Soc. Rev.*, 1998, **27**, 213–223.
- 21 I. Bilecka and M. Niederberger, *Nanoscale*, 2010, **2**, 1358–1374.
- 22 L. Liu, B. Zhang and X. J. Huang, *Progress in Natural Science-Materials International*, 2011, **21**, 211–215.
- 23 T. Azib, S. Ammar, S. Nowak, S. Lau-Truing, H. Groult, K. Zaghbi, A. Mauger and C. M. Julien, *J. Power Sources*, 2012, **217**, 220–228.
- 24 K. Nakamoto, *Infrared and Raman Spectra of Inorganic and Coordination Compounds Part A: Theory and Applications in Inorganic Chemistry*, John Wiley Inc., 5th edn, 1997, pp. 160–161.
- 25 A. V. Radha, J. D. Furman, M. Ati, B. C. Melot, J. M. Tarascon and A. Navrotsky, *J. Mater. Chem.*, 2012, **22**, 24446–24452.
- 26 N. Marx, L. Bourgeois, D. Carlier, A. Wattiaux, E. Suard, F. Le Cras and L. Croguennec, *Inorg. Chem.*, 2012, **51**, 3146–3155.
- 27 R. Malik, D. Burch, M. Bazant and G. Ceder, *Nano Lett.*, 2010, **10**, 4123–4127.